Reviews in Mineralogy & Geochemistry
Vol. 55, pp. 1-24, 2004

Overview and General Concepts

Clark M. Johnson, Brian L. Beard
Department of Geology and Geophysics
University of Wisconsin-Madison
1215 West Dayton Street
Madison, Wisconsin 53706, U.S.A.

Francis Albarède
Ecole Normale Supérieure de Lyon
46 Allée d'Italie
69007 Lyon, France

INTRODUCTION

Of the eighty-three naturally occurring elements that are not radioactive or have half lives long enough to be considered stable ($\geq 10^9$ yrs), nearly three-quarters have two or more isotopes. Variations in the isotopic ratios of a number of these elements, including H, C, N, O, and S, provide the foundation for the field of *stable isotope geochemistry*. Investigations of variations in the isotopic compositions of these *traditional* elements have provided important constraints on their sources in natural rocks, minerals, and fluids. These studies have focused on a range of problems including planetary geology, the origin and evolution of life, crust and mantle evolution, climate change, and the genesis of natural resources. Much less attention, however, has been paid to stable isotope variations of other elements that are also geochemically important such as certain metals and halogens. In part this has been due to analytical challenges, although first-order variations for several systems have been constrained using long-standing analytical methods such as gas- and solid-source mass spectrometry. With the advent of analytical instrumentation such as multi-collector, inductively-coupled plasma mass spectrometry (MC-ICP-MS), large portions of the Periodic Table are now accessible to stable isotope studies.

In this volume, the geochemistry of a number of *non-traditional* stable isotopes is reviewed for those elements which have been studied in some detail: Li, Mg, Cl, Ca, Cr, Fe, Cu, Zn, Se, and Mo. This volume is intended for the non-specialist and specialist alike. The volume touches on the multiple approaches that are required in developing new isotopic systems, including development of a theoretical framework for predicting possible isotopic fractionations, perfecting analytical methods, studies of natural samples, and establishment of a database of experimentally-determined isotope fractionation factors to confirm those predicted from theory. In addition to the systems discussed in this volume, we expect that more elements will be subject to isotopic studies in the next several years, significantly broadening the field that is known as *stable isotope geochemistry*.

Chapter 1 is intended to provide an overview of basic concepts of stable isotope geochemistry that are applicable to the chapters that follow on specific topics and isotopic systems. There are a number of excellent reviews of stable isotope geochemistry that have tended to focus on H, C, O, and S, including two prior volumes of Reviews in Mineralogy and

1529-6466/04/0055-0001$05.00

Geochemistry (Valley et al. 1986; Valley and Cole 2001), and a few texts (e.g., Criss 1999; Hoefs 2004). The concepts discussed in these works are entirely applicable to the isotopic systems discussed in the present volume. Because our discussion here is restricted to essential concepts, we refer the reader who is interested in more depth to the works above.

ISOTOPIC ABUNDANCES AND NOMENCLATURE

There are many sources for information on the distribution of the elements and isotopes (e.g., Lide 2003), as well as discussions that are pertinent to stable isotope geochemistry (e.g., Criss 1999). In Chapter 2 Birck (2004) reviews in detail the isotopic distribution and nucleosynthetic origin of many elements that are of geochemical interest. He highlights the fact that isotopic variations for many elements are greatest for extraterrestrial samples, where evidence for a variety of fractionation mechanisms and processes are recorded, including mass-dependent and mass-independent fractionation, radioactive decay, and incomplete mixing of presolar material. Below we briefly review a few general aspects of isotope distribution that are pertinent to isotopic studies that bear on nomenclature, expected ranges in isotopic fractionation, and analytical methodologies.

The number of stable isotopes for the naturally occurring elements tends to increase with increasing atomic number, to a maximum of 10 for Sn (Fig. 1). Elements with low atomic numbers tend to have the lowest number of stable isotopes, limiting the possible ways in which isotopic compositions can be reported. Both H and C have only two stable isotopes (Fig. 1), and therefore isotopic compositions are reported using one ratio, D/H and $^{13}C/^{12}C$, respectively. Single ratios can only be used for B and N, and data are reported as $^{11}B/^{10}B$ and $^{15}N/^{14}N$, respectively. Of the *non-traditional* stable isotope systems discussed in this volume, only three have just two stable isotopes (Li, Cl, and Cu; Fig. 1).

The choice of isotopic ratios for reporting data increases, of course, for elements with three or more isotopes. Although O isotope compositions are almost exclusively reported in terms

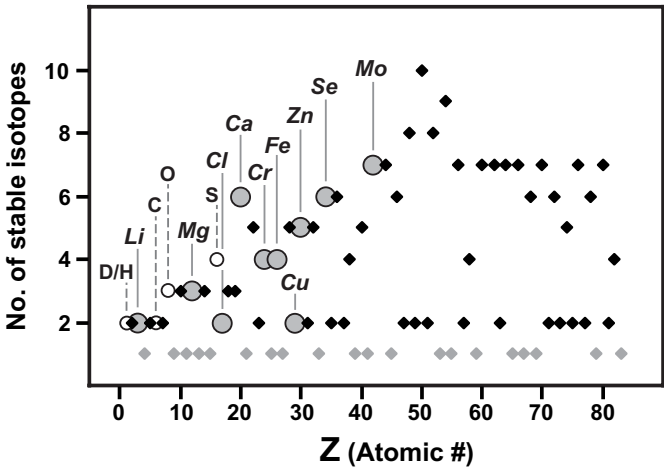

Figure 1. Number of stable isotopes relative to atomic number (Z) for the elements. Mono-isotopic elements shown in gray diamonds. Elements discussed in this volume are shown as large gray circles. Other elements that have been the major focus of prior isotopic studies are shown in small white circles, and include H, C, O, and S. Nuclides that are radioactive but have very long half-lives are also shown in the diagram.

of $^{18}O/^{16}O$ ratios, data for $^{17}O/^{16}O$ variations are reported, and are valuable in distinguishing mass-dependent and mass-independent isotopic variations (see Chapter 2; Birck 2004). The majority of S isotope data are reported using the ratio of the two most abundant isotopes, $^{34}S/^{32}S$, although studies of mass-independent isotope variations report data for three or all four stable isotopes of S (e.g., Farquhar et al. 2000). Magnesium, Ca, Cr, Fe, Zn, Se, and Mo all have three or more stable isotopes (Fig. 1), and therefore the isotopic compositions for these elements may be reported using a number of ratios. In some cases, isotopic abundances limit the isotopic ratios that can be measured with reasonable precision. For many elements, however, isotopic abundances are relatively high for a number of isotopes and, in these cases, data are reported using a number of ratios.

The vast majority of isotopic data are reported in "delta notation", where the isotopic composition is cast as the deviation of an isotopic ratio relative to the same ratio in a standard (e.g., O'Neil 1986a):

$$\delta^i E_X = \left(\frac{R_X^{i/j} - R_{STD}^{i/j}}{R_{STD}^{i/j}} \right) 10^3 \quad (1)$$

where i and j are the specific isotopes used in ratio R of element E, X is the sample of interest, and STD is a standard reference material or reservoir. It is traditional to use isotope i in the δ value, and it is important to note the specific ratio $R^{i/j}$ that is used. The units for the $\delta^i E_X$ value are in parts per thousand or "per mil", which is commonly noted using the per mil sign (‰). In the case of the $\delta^{18}O$ value, $R = {}^{18}O/{}^{16}O$, following the traditional protocol of expressing $R^{i/j}$ as the abundance ratio of the rare isotope to the major isotope (e.g., O'Neil 1986a). Similarly, δD, $\delta^{13}C$, $\delta^{15}N$ and $\delta^{34}S$ values are defined using the isotopic ratio of rare isotope over major isotope, that is, D/H, $^{13}C/^{12}C$, $^{15}N/^{14}N$, and $^{34}S/^{32}S$, respectively. The conventional definitions of $R^{i/j}$ for H, C, N, and S correspond to *heavy over light* masses, leading to a consistent nomenclature where a positive $\delta^i E_X$ value refers to a sample that is relatively enriched in the heavy isotope (a high $R^{i/j}$ ratio relative to the standard). Although some groups have reported isotopic compositions in parts per 10,000 using the ε unit (e.g., Rehkämper and Halliday 1999; Zhu et al. 2000), this nomenclature is not very common and should probably be discontinued to avoid confusion.

The standard reference used for reporting isotopic compositions of H and O is Standard Mean Ocean Water (SMOW), although the fossil marine carbonate PDB standard is also used for oxygen (O'Neil 1986a). For the new isotopic systems discussed in this volume, the choice of standard reference material or reservoirs has not been settled in many cases (Table 1), requiring careful attention when comparing $\delta^i E$ values. Some groups have chosen a major geologic reservoir such as ocean water or bulk earth, following the convention used for some light stable isotope systems, as well as several radiogenic isotope systems such as Nd, Hf, and Os. Reporting $\delta^i E$ values relative to a major geologic reservoir may be advantageous in interpretations, where relative enrichment or depletion in heavy isotopes are referenced to a geologic component. The disadvantage of using major geologic reservoirs as a reference is that they are not distinct substances that can be measured in the laboratory. In other cases, an international or other widely-available purified standard is used. For some isotopic systems, data are reported relative to in-house standards (Table 1), which may not allow easy cross-calibration with other laboratories. Data should be reported for several internationally-available standards whenever possible so that δ values may be compared using equivalent reference materials or reservoirs.

The motivation for defining the $\delta^i E_X$ value as *rare isotope over major isotope* lies in the fact that the mathematical forms of mixing relations and other physical processes are greatly simplified in cases where the rare isotope i is very low in abundance, which leads to the simplification that the abundance isotope j may be treated as invariant, particularly when the

Table 1. Nomenclature and standards for isotope systems.

Element	Ratio	Typical Precision	Standard Reference Material or Reservoir	Other Notation	Ratio	Other Standards	Isotopic Composition
δ^{7}Li (‰)	^{7}Li/^{6}Li	0.5-1.0‰	NIST SRM-8545	δ^{6}Li (‰)	^{6}Li/^{7}Li	IRMM-016	δ^{7}Li = 0
δ^{26}Mg (‰)	^{26}Mg/^{24}Mg	0.1-0.2‰	DSM 3	δ^{25}Mg (‰)	^{25}Mg/^{24}Mg	SRM 980_O	δ^{26}Mg = −3.41
				Δ^{26}Mg (non-mass-dependent variations)			
δ^{37}Cl (‰)	^{37}Cl/^{35}Cl	0.1-0.3‰	Std. Mean Ocean Chloride (SMOC)				
δ^{44}Ca (‰)	^{44}Ca/^{40}Ca	0.1-0.2‰	UCB Ca std.			Seawater Ca	δ^{44}Ca = +0.9
						Fluorite Ca	δ^{44}Ca = +0.5
				ε_{Ca} (^{40}Ca/^{42}Ca; radiogenic ^{40}Ca enrichment; parts per 10,000)			
δ^{53}Cr (‰)	^{53}Cr/^{52}Cr	0.1-0.2‰	NIST SRM-979				
δ^{56}Fe (‰)	^{56}Fe/^{54}Fe	0.1-0.5‰	Bulk Earth (BE)	δ^{57}Fe (‰)	^{57}Fe/^{54}Fe	IRMM-14	δ^{56}Fe = −0.09
				$\delta^{57/56}$Fe (‰)	^{57}Fe/^{56}Fe		
				ε^{57}Fe	^{57}Fe/^{54}Fe (parts per 10,000)		
				ε^{56}Fe	^{56}Fe/^{54}Fe (parts per 10,000)		
δ^{65}Cu (‰)	^{65}Cu/^{63}Cu	0.1-0.2‰	NIST SRM-976				
δ^{66}Zn (‰)	^{66}Zn/^{64}Zn	~0.1‰	NIST SRM-682	δ^{67}Zn (‰)	^{67}Zn/^{64}Zn	NIST SRM-683	δ^{66}Zn = +2.4
				δ^{68}Zn (‰)	^{68}Zn/^{64}Zn		
				ε^{66}Zn	^{66}Zn/^{64}Zn (parts per 10,000)		
				ε^{67}Zn	^{67}Zn/^{64}Zn (parts per 10,000)		
				ε^{68}Zn	^{68}Zn/^{64}Zn (parts per 10,000)		
δ^{80}Se (‰)	^{80}Se/^{76}Se	0.2-0.3‰	CDT	δ^{82}Se (‰)	^{82}Se/^{76}Se	NIST SRM-3149	δ^{80}Se = 0
δ^{97}Mo (‰)	^{97}Mo/^{95}Mo	0.1-0.2‰	Rochester JMC Mo	δ^{98}Mo (‰)	^{98}Mo/^{95}Mo	Seawater Mo	δ^{97}Mo = +1.5

Note: *Standard Reference Material or Reservoir* refers to $R^{i/j}_{STD}$ in equation 1 in the text.

range in isotopic compositions is relatively restricted. For example, the exact mixing relation for a single element between components *A* and *B* which differ in their isotopic compositions is given by:

$$\frac{M_A}{M_B} = -\left(\frac{C_B}{C_A}\right)\left(\frac{R^*_{MIX} - R^*_B}{R^*_{MIX} - R^*_A}\right) \tag{2}$$

where M_A and M_B are the masses of components *A* and *B*, respectively, C_A and C_B are the concentrations of the element in components *A* and *B*, respectively, and R^* is defined as the ratio of the mass of the rare isotope over the total mass of the element (Eqn. 1.14, p. 22-23, Criss 1999). In the case of O, where the abundances of ^{18}O and ^{16}O are 0.20% and 99.76%, respectively, R^* is very nearly equal to the $^{18}O/^{16}O$ ratio, allowing us to relate the exact mixing equation directly to the measured isotopic compositions. We may further simplify Equation (2) using δ notation as:

$$\delta^i E_{MIX} \approx \delta^i E_A f + \delta^i E_B (1 - f) \tag{3}$$

where *f* is the fraction of component *A* in the two-component mixture.

Although the simplicity of Equation (3) makes it quite useful, it is important to note that it is valid only for cases when the abundance of the isotope in the numerator of *R* is very low or when the difference between $\delta^i E_A$ and $\delta^i E_B$ is small. For example, use of Equation (3) for mixing two components that differ in their $^{18}O/^{16}O$ ratios by 50‰ produces an error of 0.0016‰ at 50:50 mixing (assuming equal oxygen abundances) relative to use of the exact mixing Equation (2). However, in the case of Fe isotopes, for example, where ^{56}Fe and ^{54}Fe have abundances of 91.76% and 5.84%, respectively, the assumption that ^{54}Fe is a rare isotope is not valid. Assuming that two components differ in their $^{56}Fe/^{54}Fe$ ratios by 50‰, use of the approximate Equation (3) produces an error of 0.61‰ at 50:50 mixing (assuming equal iron abundances) relative to use of the exact mixing Equation (2). If mixing relations are calculated using $^{57}Fe/^{54}Fe$ ratios, as is reported by a number of workers, isotope *i* is even closer in abundance to isotope *j*, and the error introduced using Equation (3) in the above example becomes larger, at 0.90‰. Fortunately, we will see that except for Li, isotopic variations in nature for the elements discussed in this volume are generally less than 10‰, and in most cases Equation (3) may be used without significant loss in accuracy. This may not be the case, however, for experiments that involve enriched isotope tracers.

It is not always possible to follow the convention of *rare isotope over major isotope* in the definition of $\delta^i E_X$ *and* maintain the convention *heavy over light* for elements across the Periodic Table. If we restrict *R* to be the ratio of the major isotope to the next-most-abundant isotope, it will be *heavy over light* for only half of the elements under consideration (Fig. 2). The combined definition of *rare over major* and *heavy over light* is satisfied for Mg, Cl, Ca, Cr, Cu, and Zn, but is *not* satisfied for Li, Fe, Se, and Mo (Fig. 2). If the *rare over major* definition of *R* is maintained, as has been the norm for over five decades of work in the *traditional* stable isotopes, then there will be inconsistencies in the sign of the $\delta^i E_X$ value, where, in some cases, a positive value will reflect a relative enrichment in the heavy isotope, and in others, a depletion. Given the fact that some nucleosynthetic processes produce values of *R* (as defined in Fig. 2) that approach unity with increasing atomic number (Fig. 2), we suggest that the isotope community should abandon the practice of *rare over major* in defining *R* for new isotopic systems at the intermediate- to heavy-mass range, because as *R* approaches unity, the simplifications of mixing and other equations become less accurate, regardless of defining isotopic ratios as *rare over major* or *major over rare*. Instead, defining *R* for new isotopic systems as *heavy over light* is probably preferred, because this will maintain the same convention used in *traditional* stable isotope systems, where a positive $\delta^i E_X$ value

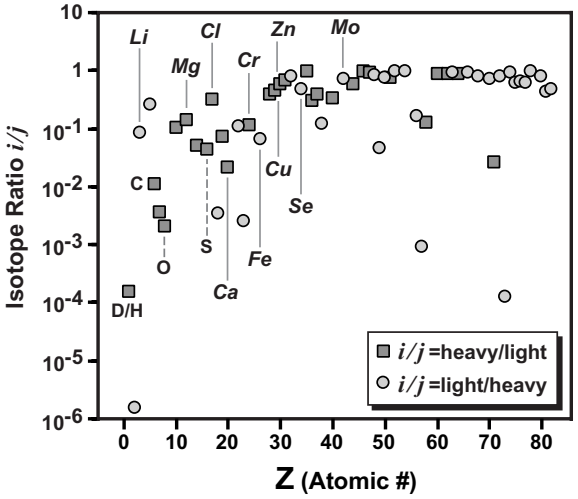

Figure 2. Variations in isotope ratio *i*/*j* for elements that have two of more isotopes relative to atomic number (Z), where *j* is the most abundant mass, and *i* is the next-most abundant mass. Elements where *i*/*j*, as defined here, reflects the ratio of a heavy mass *i* relative to that of *j* are shown in gray squares, whereas elements where *i*/*j* reflects a lighter mass *i* over heavy mass *j* are shown in gray circles. The lighter elements tend to have low *i*/*j* ratios, from ~10^{-6} to ~10^{-1}, which simplify mixing relations in terms of δ plots. In the case of elements that have been extensively studied for their isotopic variations, such as H, C, O, and S, *i*/*j* is heavy over light, leading to the traditional convention that a high δ value reflects a relative enrichment of the heavy isotope. The convention *i*/*j* does not remain consistently *heavy over light* for a number of non-traditional stable isotopes, including those discussed here.

indicates a relative enrichment in the heavy isotope relative to a standard (or, more precisely, an enrichment in the heavy/light isotopic *ratio*, as discussed above), and a negative $\delta^i E_X$ value indicates a relative depletion in the heavy isotope. The *heavy over light* convention is followed in this volume.

ISOTOPIC FRACTIONATIONS

As discussed by O'Neil (1986b), and also in Chapter 3 of this volume (Schauble 2004), isotopic fractionations between species or phases depend on a number factors, including relative mass difference, the nature of the bonding environment, and redox state. Ignoring issues related to bonding and redox state, we generally expect that the range in isotopic variations will decrease with increasing atomic number (*Z*) because the relative mass difference also decreases (Fig. 3), generally following the relation of 1/*Z*. The relatively large mass differences for the *traditional* stable isotopes such as H, C, O, and S, ranging from 66.7% for H to 3.0% for S (calculated as $\Delta m/\bar{m}$; Fig. 3), are in part responsible for the large ranges in isotopic ratios that have been measured in natural samples for these elements, from 10's to 100's of per mil (‰). As reviewed in Chapter 5 (Tomascak 2004), of the elements discussed in this volume, Li shows the greatest range in isotopic composition, commensurate with its low mass, high relative mass difference, and bonding environment (Fig. 3). Despite relatively small mass differences on the order of ~1%, however, significant isotopic variations are seen up through Mo (Chapter 12), and, in fact, are seen for heavier elements such as Hg (*Z* = 80; Jackson 2001) and Tl (*Z* = 81; Rehkämper et al. 2002), indicating that new isotopic systems are likely to be developed across the Periodic Table as analytical precision improves, even for

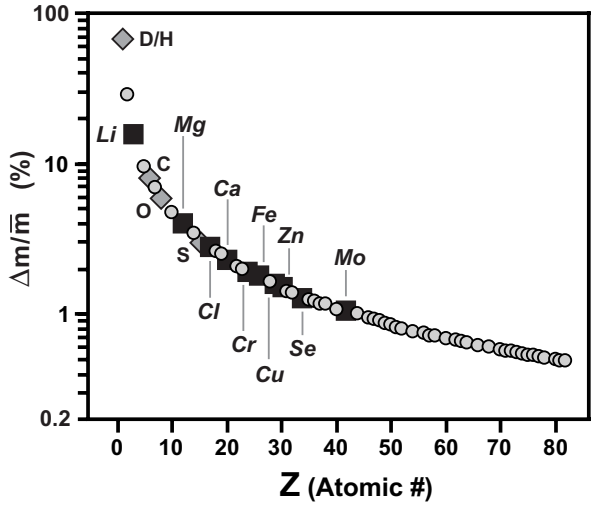

Figure 3. Relative mass differences for elements that have two or more isotopes, cast as $\Delta m/\bar{m}$, where Δm is the unit mass difference ($\Delta m = 1$), and $\bar{m}$ is the average mass of the isotopes of that element, as a function of atomic number (Z). Note that $\Delta m/\bar{m}$ is reported in percent, and is plotted on a log scale. Elements that are discussed in this volume shown in large black squares. Other elements that have been the major focus of isotopic studies shown in gray diamonds, and include H, C, O, and S. The relatively large mass differences for the light elements generally produce the largest isotopic fractionations, whereas the magnitude of isotopic fractionation is expected to markedly decrease with increasing mass.

heavy elements where the relative mass differences are only a few tenths of a percent.

The relatively small mass differences for most of the elements discussed in this volume requires very high-precision analytical methods, and these are reviewed in Chapter 4 by Albarède and Beard (2004), where it is shown that precisions of 0.05 to 0.2 per mil (‰) are attainable for many isotopic systems. Isotopic analysis may be done using a variety of mass spectrometers, including so-called *gas source* and *solid source* mass spectrometers (also referred to as *isotope ratio* and *thermal ionization* mass spectrometers, respectively), and, importantly, MC-ICP-MS. Future advancements in instrumentation will include improvement in *in situ* isotopic analyses using ion microprobes (secondary ion mass spectrometry). Even a small increase in precision is likely to be critical for isotopic analysis of the intermediate- to high-mass elements where, for example, an increase in precision from 0.2 to 0.05‰ could result in an increase in signal to noise ratio from 10 to 40.

The isotope fractionation factor and mass-dependency of fractionation

Following standard practice (e.g., O'Neil 1986a), the isotopic fractionation factor between two substances A and B is defined as:

$$\alpha_{A\text{-}B} = \frac{R_A^{i/j}}{R_B^{i/j}} \tag{4}$$

which may be cast in terms of $\delta^i E$ values as:

$$\alpha_{A\text{-}B} = \frac{1000 + \delta^i E_A}{1000 + \delta^i E_B} \tag{5}$$

Note that $\alpha_{A\text{-}B}$ simply reflects the contrast in isotopic compositions between two substances and, in terms of physical processes, could reflect equilibrium or non-equilibrium partitioning of isotopes. For an isotope exchange reaction in which one atom is exchanged, $\alpha_{A\text{-}B}$ is equal to the equilibrium constant. Because $\alpha_{A\text{-}B}$ is very close to unity, generally on the order of $1.00X$, we may take advantage of the relation that $10^3\ln(1.00X) \approx X$, which provides the useful relation:

$$10^3 \ln \alpha_{A\text{-}B} \approx \delta^i E_A - \delta^i E_B \equiv \Delta_{A\text{-}B} \tag{6}$$

This allows us to describe isotopic fractionations by simply subtracting the $\delta^i E$ values of substances A and B (carefully keeping the order of subtraction consistent). Assuming a fractionation of 10‰ ($\alpha_{A\text{-}B} = 1.010$), an error of only 0.05‰ is introduced if the fractionation is described using $\Delta_{A\text{-}B}$ as compared to $\alpha_{A\text{-}B}$, which will be immaterial for most of the elements discussed in this volume, unless the fractionations are very large (several tens of per mil or greater).

Isotopic fractionations are sometimes discussed using the ε notation, and this has been most commonly used to describe kinetic isotope effects. This usage is common in the S isotope literature (e.g., Canfield 2001), and is also used in Chapter 9 (Johnson and Bullen 2004). The fractionation between reactant A and product B is defined as:

$$\varepsilon_{A\text{-}B} = \left(\alpha_{A\text{-}B} - 1\right)\ 10^3 \tag{7}$$

$\varepsilon_{A\text{-}B}$ therefore has units of per mil.

For elements that have three or more isotopes, isotopic fractionations may be defined using two or more isotopic ratios. Assuming that isotopic fractionation occurs through a mass-dependent process, the extent of fractionation will be a function of the relative mass differences of the two isotope ratios. For example, assuming a simple harmonic oscillator for molecular motion, the isotopic fractionation of $R^{i/j}$ may be related to $R^{k/j}$ as:

$$\alpha_{k/j} = \left(\alpha_{i/j}\right)^Z \tag{8}$$

where $Z = (m_i/m_k)\{(m_k - m_j)/(m_i - m_j)\}$, and m refers to the masses of the individual isotopes i, j, and k (e.g., Criss 1999). We illustrate this mass-dependent relation for Mg in Figure 4, where Equation (8) becomes:

$$\alpha_{25/24} = (\alpha_{26/24})^{0.521} \tag{9}$$

Over small ranges in isotopic composition, Equation (8) may be approximated by the linear form:

$$\delta^k E \approx \left(\frac{k-j}{i-j}\right) \delta^i E \tag{10}$$

where i, j, and k are integer masses. In the case of Mg, this relation would be:

$$\delta^{25}\mathrm{Mg} \approx 0.5\ \delta^{26}\mathrm{Mg} \tag{11}$$

Equations (8) and (10) are applicable to stable isotope systems where isotopic fractionation occurs through mass-dependent processes which comprise the majority of cases described in this volume. These relations may also be used to identify mass-independent fractionation processes, as discussed in Chapter 2 (Birck 2004). Mass-dependent fractionation laws other than those given above distinguish equilibrium from kinetic fractionation effects, and these are discussed in detail in Chapters 3 and 6 (Schauble 2004; Young and Galy 2004). Note that distinction between different mass-dependent fractionation laws will generally require very

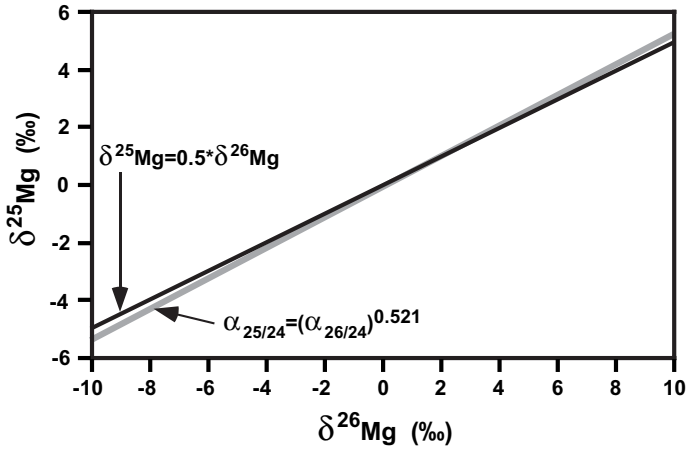

Figure 4. Illustration of mass-dependent fractionation of Mg isotopes, cast in terms of δ values. δ^{26}Mg and δ^{25}Mg values based on ^{26}Mg/^{24}Mg and ^{25}Mg/^{24}Mg ratios, respectively. A common equilibrium fractionation model, as defined by exponential relations between α values (fractionation factors) for different isotope ratios, is shown in the gray line. A simple linear relation, where the slope is proportional to the mass difference of the isotope pair, is shown in the black line. Additional mass-dependent fractionation laws may be defined, and all are closely convergent over small ranges (a few per mil) in isotope compositions at δ values that are close to zero.

high-precision isotopic analyses, depending on the range in isotopic compositions that are produced (Chapters 4 and 6).

The choices for defining $\delta^i E$ values for new isotope systems that contain multiple isotopes will be largely determined by consideration of the analytical precision. For example, Ca isotope ratios might be reported using the extreme end members ^{40}Ca and ^{48}Ca, representing an 8 mass-unit spread. But, as discussed in Chapter 8, the very low abundance of ^{48}Ca (0.19%) makes this a poor choice. Although ^{44}Ca/^{40}Ca fractionations are one-half those of ^{48}Ca/^{40}Ca fractionations, the much higher precision with which the ^{44}Ca/^{40}Ca ratio may be determined makes this ratio a superior choice. In the case of Mg, where the two minor isotopes ^{25}Mg and ^{26}Mg have nearly equal abundances of 10.00% and 11.01%, respectively, ^{25}Mg/^{24}Mg and ^{26}Mg/^{24}Mg ratios should be determined with equal precision, making the ^{26}Mg/^{24}Mg ratio the clear choice for providing the largest signal to noise ratio because ^{26}Mg/^{24}Mg fractionations will be approximately twice those of ^{25}Mg/^{24}Mg fractionations for mass-dependent processes. In practice, however, both ratios are commonly measured to provide insight into different mass-dependent processes, as well as monitor possible anomalies in ^{26}Mg abundances due to decay of ^{26}Al, which may be an issue for extraterrestrial samples; these issues are discussed in detail in Chapters 2 and 6 (Birck 2004; Young and Galy 2004).

Predicted and measured isotopic variations

The general "rules of thumb" for isotopic fractionations discussed in Chapter 3 (Schauble 2004), including bonding, redox state, and relative mass differences, lay out broad expectations for the extent of isotopic fractionations that may be observed in new isotopic systems. Several examples of isotopic fractionations for various elements are illustrated in Figure 5. Commensurate with its large relative mass difference, ^{18}O/^{16}O fractionations may be quite large at low temperatures, exceeding, for example 20‰ for $CaCO_3$–H_2O fractionations at 50°C (Fig. 5). Although isotopic fractionations are relatively large at low temperatures

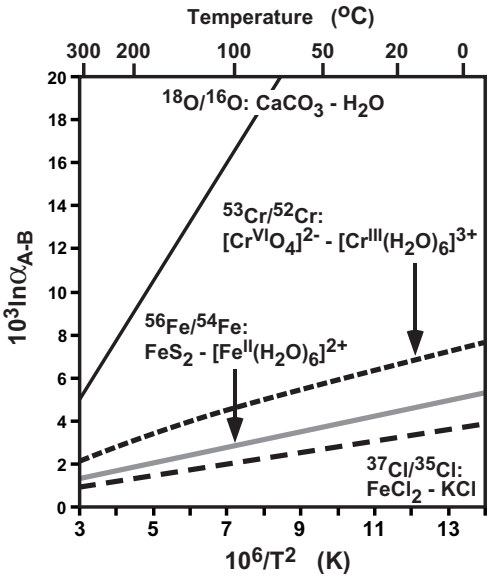

Figure 5. Examples of predicted and measured isotopic fractionations for O, Cr, Fe, and Cl, as cast in the traditional $10^3 \ln\alpha_{A-B}$ - $10^6/T^2$ diagram. The quantity $10^3 \ln\alpha_{A-B}$ places the isotope fractionation factor α_{A-B} in units of per mil (‰). Isotopic fractionations for relatively light elements, such as O, are generally higher than those of higher-mass elements, as expected based on changes in their relative mass differences (Fig. 3). $CaCO_3$ - H_2O curve for $^{18}O/^{16}O$ fractionations based on experiments from O'Neil et al. (1969). $[Cr^{VI}O_4]^{2-}$ - $[Cr^{III}(H_2O)_6]^{3+}$ curve for $^{53}Cr/^{52}Cr$ fractionations based on calculations from Schauble et al. (2004). FeS_2 - $[Fe^{II}(H_2O)_6]^{2+}$ curve for $^{56}Fe/^{54}Fe$ fractionations based on calculations from Polyakov and Mineev (2000) and Schauble et al. (2001). $FeCl_2$ - KCl curve for $^{37}Cl/^{35}Cl$ fractionations based on calculations by Schauble et al. (2003).

they are generally much smaller for higher-mass elements, where they are rarely expected to exceed 10‰ at temperatures of 100°C or less. For example, calculations of $^{37}Cl/^{35}Cl$, $^{53}Cr/^{52}Cr$, and $^{56}Fe/^{54}Fe$ fractionations for the systems $FeCl_2$–KCl, $Cr(VI)_{aq}$–$Cr(III)_{aq}$, and FeS_2–$Fe(II)_{aq}$, respectively, range from 1 to 5‰ at 100°C (Fig. 5; Schauble 2004). Although these isotopic fractionations are significantly smaller than those found for H, C, O, and S, they are still significant relative to current state-of-the-art analytical precisions (Chapter 4; Albarède and Beard 2004).

In Figure 6 we summarize the range in isotopic compositions measured for natural terrestrial samples for the elements discussed in this volume (Li, Cl, Ca, Cr, Fe, Cu, Zn, Se, and Mo). As discussed in Chapter 2, as well as in several subsequent chapters, the range in isotopic compositions for many of these elements is extended considerably if extraterrestrial samples are included. The very large relative mass difference of 15% for ^6Li and ^7Li has produced a very large range in isotopic compositions in nature of ~75‰ (Fig. 6). As reviewed in Chapter 6 (Tomascak 2004) the largest Li isotope fractionation is produced in relatively low-temperature environments, including seafloor weathering and marine hydrothermal systems. Most igneous rocks have relatively homogenous δ^7Li values, unlike other light isotopes such as those of oxygen, suggesting that larger fractionations are associated with covalently bonded O in silicates as compared to the ionic bonds that characterize Li. The isotopes of Mg have one-third of the relative mass difference of Li, but, so far, the range in $\delta^{26}Mg$ values are proportionally much smaller than suggested by the contrast in relative mass differences of the two elements (Fig. 6). $\delta^{26}Mg$ values for Mg-bearing carbonates appear to vary by ~2‰, but little is yet known about Mg isotope fractionations at low temperatures. Because Mg is a light element which has two of its three isotopes that are similar in abundance, it is ideally suited to investigation of different mass-dependent fractionation mechanisms that may operate in nature, and Young and Galy (2004) discuss this in detail in Chapter 6.

Chlorine isotope compositions vary by up to 15‰ (Chapter 7; Stewart and Spivack 2004). These large variations in Cl isotope compositions are found in marine environments, including mid-ocean ridge basalts, seafloor and hydrothermal alteration products, and sedimentary pore

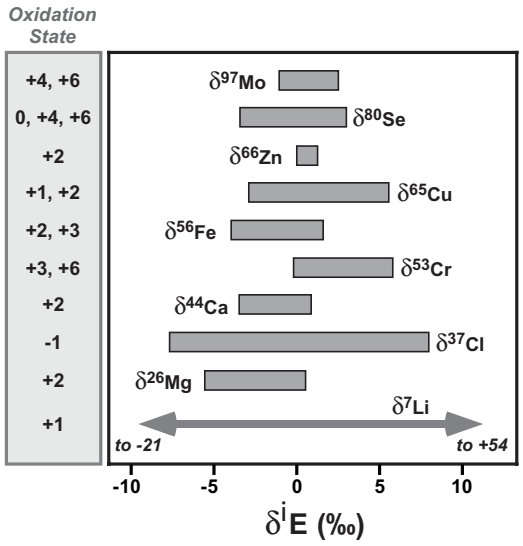

Figure 6. Summary of ranges in isotopic compositions for natural terrestrial samples as discussed in this volume. Isotopic variability in extraterrestrial samples is often greater. Isotopic compositions reported as δ values in units of per mil (‰), based on isotopic ratios and reference standards as used in this volume (Table 1). Note that the range of isotopic compositions for Li is much greater than the scale used in the diagram, where δ^7Li values vary from −21 to +54. In many cases, relatively large isotopic fractionations occur during redox reactions (see Chapter 3), and the common oxidation states in near-surface natural environments are listed on the left.

fluids. δ^{37}Cl values of fumarolic gases are also quite variable, suggesting a potential genetic tracer. Stewart and Spivack (2004) also note that significant Cl isotope variations are found in chlorinated organic compounds produced by industrial processing, similar to those found for industrially processed Li. These observations highlight the potential environmental applications of Li and Cl isotope variations.

Mantle-derived igneous rocks appear to be homogenous with respect to mass-dependent Ca isotope variations, although some K-rich rocks may have anomalously low δ^{44}Ca values reflecting ^{40}Ca enrichments from ^{40}K decay (Chapter 8; DePaolo 2004). One of the more important contrasts in Ca isotope compositions in the Earth is that measured between seawater Ca and igneous Ca, which appears to reflect Ca isotope fractionation during weathering and transport to the oceans. In contrast to the relatively high δ^{44}Ca values for seawater, biologically-processed Ca has relatively low ^{44}Ca/^{40}Ca ratios, and this appears to systematically decrease up the food chain. These observations highlight the potential for using Ca isotopes to trace biological processing of Ca in higher-order animals.

The isotope geochemistry of two redox-sensitive elements, Cr and Se, are compared in Chapter 9 by Johnson and Bullen (2004). Because Cr(VI) is quite soluble in natural waters, and is highly toxic, the significant fractionation in ^{53}Cr/^{52}Cr ratios that occurs during redox cycling of Cr is likely to find wide application in environmental geochemistry. Production of high δ^{53}Cr values for aqueous Cr seems likely to be a fingerprint for chromium reduction in natural systems. Selenium commonly occurs in three oxidation states in near-surface natural environments, Se(0), Se(IV), and Se(VI), and thus it is not surprising that significant isotopic fractionations are observed during redox cycling. The largest Se isotope fractionations appear to occur during reduction of Se(VI) and Se(IV) oxyanions, and this may occur through microbial activity, or through abiotic reduction.

Iron isotope geochemistry is reviewed in Chapter 10A (Beard and Johnson 2004) where summaries are given of the variations in ^{56}Fe/^{54}Fe ratios in inorganic experimental systems and natural igneous, metamorphic, and sedimentary rocks. Large fractionations of ^{56}Fe/^{54}Fe ratios occur during redox cycling of Fe, where low δ^{56}Fe values appear to be characteristic of reducing near-surface environments. In contrast, terrestrial surface weathering does not

appear to fractionate Fe isotopes for bulk sedimentary materials, although isotopic variations during hydrothermal alteration of oceanic crust is well documented. Significant Fe isotope variations are also found in some high-temperature samples. In Chapter 10B, Johnson et al. (2004) discuss experimental evidence for biological fractionation of Fe isotopes, during microbial reduction and oxidation, as well as supporting studies in mineral dissolution and sorption. Microbial reduction of ferric oxides produces aqueous Fe(II) that has low δ^{56}Fe values whose origin lies in a number of pathways, whereas microbial oxidation produces ferric Fe precipitates that have relatively high δ^{56}Fe values.

Review of the isotope geochemistry of the transition metals is continued by Albarède (2004) in Chapter 11, where isotopic variations in Cu and Zn are discussed. The significant changes in bonding environments of Cu(I) and Cu(II) produce significant differences in δ^{65}Cu values for oxidized and reduced Cu compounds, and isotopic variations of up to 9‰ are observed in nature. Isotopic variations of Zn are significantly more restricted, where δ^{66}Zn values vary by less than 2‰, but systematic variations are recorded in Fe–Mn nodules from the ocean floor. Measurable isotopic variations are found for Cu and Zn in sedimentary rocks, as well as ore deposits, and this remains a promising aspect of future Cu and Zn isotope studies.

Molybdenum isotope variations appear to be on the order of 3.5‰ in ^{97}Mo/^{95}Mo ratios, where the largest fractionation is seen between aqueous Mo in seawater and that incorporated in Fe–Mn crusts and nodules on the seafloor (Chapter 12; Anbar 2004). This isotopic contrast is interpreted to reflect fractionation by Mo sorption to Mn oxide-rich sediments relative to aqueous Mo. The δ^{97}Mo values for euxinic sediments in turn are distinct from those of Fe–Mn crusts, highlighting the isotopic contrasts between major repositories of Mo in surface and near-surface environments. As discussed by Anbar (2004) in Chapter 12, a major focus of research on Mo isotopes has been the potential use as a paleoredox indicator in marine systems.

Processes that may produce isotopically distinct reservoirs

We briefly review processes in which isotopic fractionations may be recorded in isotopically distinct reservoirs that are preserved in nature. These concepts have been extensively covered in the H, C, O, and S isotope literature, and we illustrate several examples for the *non-traditional* stable isotope systems discussed in this volume. One of the simplest processes that produces isotopically distinct reservoirs would be slow reaction of substance A to B, where A and B remain open to complete isotopic exchange during the process. This is commonly referred to as *closed system equilibrium*, and the changes in isotopic compositions that occur may be defined by the exact relation:

$$\delta^i E_B = \frac{\alpha_{B\text{-}A}\,\delta^i E_{SYS} + 1000 f\left(\alpha_{B\text{-}A} - 1\right)}{\alpha_{B\text{-}A} - \alpha_{B\text{-}A} f + f} \tag{12}$$

where $\alpha_{B\text{-}A}$ is the *B-A* fractionation factor, $\delta^i E_{SYS}$ is the $\delta^i E$ value for the total system, and f is the fraction of *A* remaining ($f = 1$ when the system is entirely *A*) (Eqn. 3.19, p. 105, Criss 1999). Note that Equation (12) is simpler if cast in terms of $\alpha_{B\text{-}A}$ rather than $\alpha_{A\text{-}B}$, as was defined in Equation (4) above. If $\alpha_{B\text{-}A}$ is close to unity, Equation (12) may be simplified to:

$$\delta^i E_B \approx \delta^i E_{SYS} + f\left(\alpha_{B\text{-}A} - 1\right) 10^3 \tag{13}$$

(Criss 1999), which may be further simplified to:

$$\delta^i E_B \approx \delta^i E_{SYS} + f\,\Delta_{B\text{-}A} \tag{14}$$

using the approximation $\Delta_{B\text{-}A} \approx (\alpha_{B\text{-}A} - 1) \times 10^3$ (note that this is equivalent to $\varepsilon_{B\text{-}A}$, following Eqn. 7 above). Following these simplifications, the corresponding $\delta^i E_A$ value, at a given *f*, is:

$$\delta^i E_A \approx \delta^i E_B - \Delta_{B\text{-}A} \tag{15}$$

(Criss 1999). Equations (14) and (15) describe a straight line in terms of $\delta^i E_A$ or $\delta^i E_B$ as a function of *f* or the fraction of *B* produced (Fig. 7). For example, in a system that is initially composed only of *A* and has an initial $\delta^i E$ value of zero, where $10^3 \ln\alpha_{B\text{-}A} \approx \Delta_{B\text{-}A} = -1.5‰$, the first fraction of B to form will have $\delta^i E_B = -1.5‰$ (Fig. 7). As the reaction proceeds, the shifting mass balance of phases *A* and *B* will require shifts in their $\delta^i E$ values while maintaining a constant isotopic fractionation between *A* and *B* (Fig. 7). When the reaction is

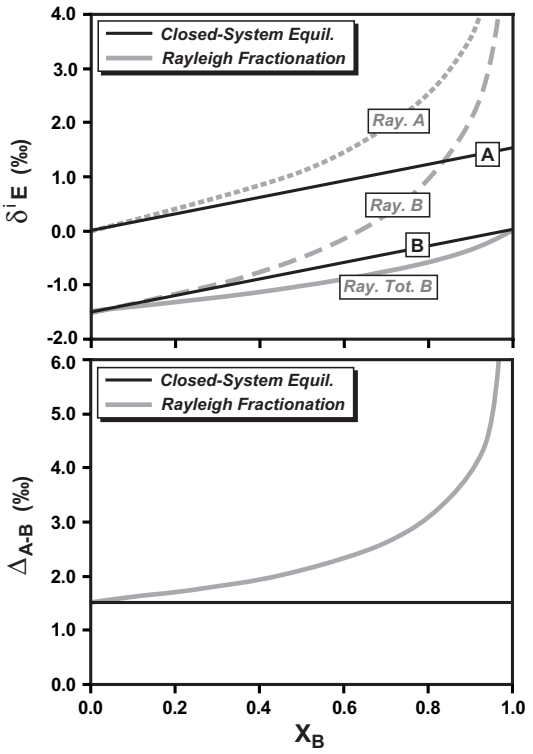

Figure 7. Comparison of isotopic fractionations produced by closed-system equilibrium and Rayleigh fractionation processes where phase *A* is reacted to phase *B*, as a function of the proportion of *B* (X_B) that is produced. Isotopic compositions are reported as $\delta^i E$, in units of per mil, and the fractionation factor $\alpha_{B\text{-}A}$ is 0.9985 ($\alpha_{A\text{-}B}$=1.0015). In the upper diagram, solid black lines mark the $\delta^i E$ values of reactant *A* and product *B* that reflect the isotopic mass-balance constraints imposed by a closed system where *A* and *B* continuously maintain isotopic equilibrium. During Rayleigh fractionation (gray lines), the product *B* is isolated from isotopic exchange with A immediately after formation, producing more extreme isotopic variations than in closed-system equilibrium fractionation. The $\delta^i E$ values of remaining phase *A* are shown in the short-dashed line in the upper diagram, and the $\delta^i E$ values of the instantaneous product *B* is shown in the long-dashed lines in the upper diagram. Variations in the $\delta^i E$ values for the *total product B* shown in solid gray line. In the lower diagram, the measured isotopic contrast between *A* and *B*, which may be conveniently defined as $\Delta_{A\text{-}B}$ (see text), is constant for closed-system equilibrium fractionation (solid horizontal line), but changes during Rayleigh fractionation (curved gray line), even for a constant fractionation factor $\alpha_{A\text{-}B}$ that may reflect equilibrium conditions.

complete and the system is entirely B, mass balance requires that $\delta^i E_B$ is the same as the initial $\delta^i E_A$ value (Fig. 7). The importance of this illustration is that in cases where reactions go to completion, if there is no addition or loss of element E from the system, there will be no net change in isotopic composition, even if $\alpha_{B\text{-}A}$ is significantly different than unity. Although data that fall along linear $\delta^i E - f$ trends are likely to be indicative of isotopic equilibrium, there are cases where incremental (Rayleigh) fractionation may occur under kinetic conditions that may be mistaken for closed-system equilibrium (e.g., p. 154-157, Criss 1999), requiring other approaches to establishing isotopic equilibrium such as use of enriched isotope tracers.

In the case of reactions where the products do not continue to exchange with other phases in the system, as might be the case during precipitation of a mineral from solution, Rayleigh fractionation may best describe the changes in $\delta^i E$ values for the individual components. The well-known Rayleigh equation (Rayleigh 1902) is:

$$\frac{\left[R^{i/j}\right]}{\left[R^{i/j}\right]_{\mathrm{i}}} = f^{(\alpha_{B\text{-}A}-1)} \tag{16}$$

where $[R^{i/j}]_{\mathrm{i}}$ is the initial ratio $R^{i/j}$ (which may be defined for either A or B), and f is the fraction of A remaining. Cast in terms of $\delta^i E$ values, Equation (16) becomes:

$$(1000 + \delta^i E)/(1000 + \delta^i E_{\mathrm{i}}) = f^{(\alpha_{B\text{-}A}-1)} \tag{17}$$

where $\delta^i E$ may be defined for either A or B, and the subscript i refers to the initial $\delta^i E$ value.

The products of Rayleigh fractionation are effectively isolated from isotopic exchange with the rest of the system immediately upon formation. If the process occurs slowly, such that each increment of product B forms in isotopic equilibrium with the reactant A prior to isolation of B from the system, then $\alpha_{B\text{-}A}$ would be an equilibrium isotope fractionation factor. However, if the process of formation of B is rapid, incremental formation of B may be out of isotopic equilibrium with A. In this case, $\alpha_{B\text{-}A}$ would be a kinetic isotope fractionation factor, which may be a function of reaction rates or other system-specific conditions.

Because the product in Rayleigh fractionation is progressively isolated, large changes in $\delta^i E$ values in the remaining components may occur (Fig. 7). A common process by which this occurs would be condensation or precipitation. Assuming that $\alpha_{B\text{-}A}$ is constant, the differences in the instantaneous $\delta^i E$ values for A and incremental formation of B will be constant (Fig. 7). However, in practice, the isotopic composition of the *total* condensed or solid phase after a given extent of reaction is of interest, and the changes in $\delta^i E$ values for the total phase B are more modest than for the incremental portions of B (Fig. 7). Because the $\delta^i E$ values of the remaining reactant A change dramatically toward the end of the reaction, the apparent value of $\Delta_{B\text{-}A}$ between A and the *total* condensed or solid phase deviates strongly from the fractionation factor as the reaction proceeds, and this is a key feature of Rayleigh fractionation (Fig. 7). As can be seen in Figure 7, the difference in the measured $\delta^i E$ values for A and total B most closely match that of the true fractionation factor at the beginning of the reaction, where the measured isotopic contrast is insensitive to the specific mechanism (e.g., closed-system equilibrium or Rayleigh) by which A and B are physically separated (Fig. 7).

Adsorption of Mo to Mn oxyhydroxides produces an isotopic fractionation that appears to follow that of a closed-system equilibrium model as a function of the fraction of Mo adsorbed (Fig. 8). Barling and Anbar (2004) observed that the δ^{97}Mo values for aqueous Mo (largely the $[MoO_4]^{2-}$ species) were linearly correlated with the fraction (f) of Mo adsorbed (Fig. 8), following the form of Equation (14) above. The δ^{97}Mo–f relations are best explained by a Mo_{aq}–Mn oxyhydroxide fractionation of +1.8‰ for ^{97}Mo/^{95}Mo, and this was confirmed through isotopic analysis of three solution-solid pairs (Fig. 8). The data clearly do not lie

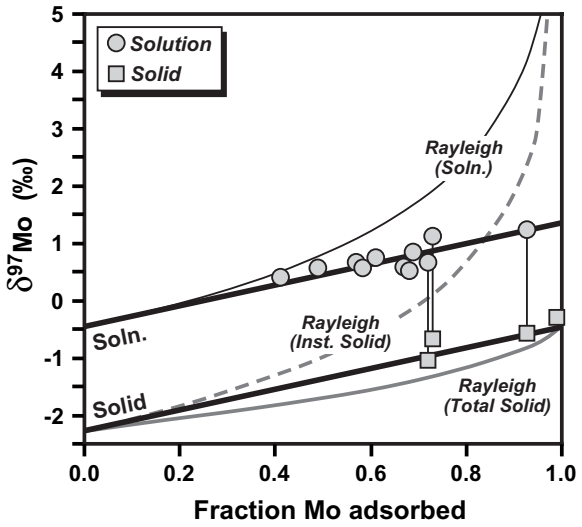

Figure 8. Example of apparent closed-system equilibrium fractionation, where Mo in solution is sorbed to Mn oxides (Barling and Anbar 2004). The δ^{97}Mo values of the Mo remaining in solution during sorption follow the linear trends that are consistent with closed-system equilibrium fractionation where isotopic equilibrium is continuously maintained between Mo in solution and that sorbed to the Mn oxides. Three aqueous-solid pairs (shown with tie lines) are consistent with this interpretation. The isotopic data cannot be explained through a Rayleigh process, where the product of the reaction (sorbed Mo) is isolated from isotopic exchange with aqueous Mo.

along a Rayleigh fractionation trend (Fig. 8), as would be expected if the adsorbed Mo did not remain in isotopic communication with Mo_{aq} at different degrees of total adsorption.

In contrast, reduction of Cr(VI) in solution, followed by precipitation of hydrated $Cr^{III}_2O_3$, produces fractionation in $^{53}Cr/^{52}Cr$ that follows a Rayleigh process (Fig. 9). When plotted as a function of the fraction of $Cr(VI)_{aq}$ reduced (f), the δ^{53}Cr values increase non-linearly, lying about a Rayleigh fractionation trend calculated for a $[Cr^{VI}O_4]^{2-}$–hydrous $Cr^{III}_2O_3$ fractionation of +3.4‰ (Fig. 9). The δ^{53}Cr–f trends are not consistent with the linear trends expected for a closed-system equilibrium model. In the Cr(VI) reduction experiments of Ellis et al. (2002), the fractionation factor, $\alpha_{Cr(VI)-Cr(III)}$, derived from the data is interpreted to reflect kinetic isotope fractionation, although it is important to note that not all Rayleigh processes are associated with kinetic isotope fractionation.

DETERMINATION OF ISOTOPIC FRACTIONATION FACTORS

Isotopic fractionation factors may be calculated based on theory (e.g., Urey 1947; Bigeleisen and Mayer 1947), and the various approaches used for such calculations are discussed in detail in Chapter 3 (Schauble 2004). Calculated fractionation factors are extremely important for new isotope systems because they constrain the isotopic fractionations that may be anticipated in nature, and, in some cases, provide the only means for constraining fractionation factors for systems that are inaccessible to experiments. Isotopic fractionation factors may also be inferred from natural assemblages (e.g., Bottinga and Javoy 1975), although issues of attainment of isotopic equilibrium or differential exchange upon cooling remain in many cases (e.g., Giletti 1986; Eiler et al. 1992; Kohn and Valley 1998). Ultimately, however, experimental verification of calculated fractionation factors is desirable. In their compilation of experimentally determined isotope fractionation factors for H, C, and O isotopes, Chacko et al. (2001) summarize measurements for 306 systems, many of which involved several independent studies. We are far from reaching this level of experimental calibration of isotope fractionation factors for the new isotopic systems discussed in this volume, and expanding the database of isotope fractionation factors remains a high priority for the isotope community.

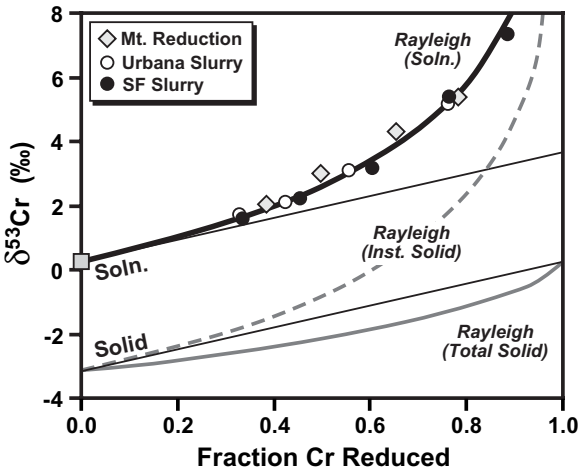

Figure 9. Example of Rayleigh fractionation produced during reduction of aqueous Cr(VI) to Cr(III), as reported in three reduction experiments by Ellis et al. (2002). Because the reduced product is a Cr(III)-hydroxide that does not continue to isotopically exchange with the aqueous Cr(VI), the δ^{53}Cr values of the remaining Cr(VI) increase along a Rayleigh trend. Although each of the three experiments of Ellis et al. (2002) produced slightly different Cr(III)-Cr(VI) fractionation factors, the curves illustrated are calculated for a single $\alpha_{Cr(III)-Cr(VI)}$=0.9966. Ellis et al. (2002) interpret the inferred $\alpha_{Cr(III)-Cr(VI)}$ as reflecting kinetic isotope fractionation during reduction and precipitation.

The majority of experimental studies of isotope fractionation have involved fluid-mineral pairs, reflecting the common means by which minerals form, particularly in low-temperature environments. In fluid-mineral systems, isotopic exchange is limited by the exchange properties of the solid phase, where the mechanisms of exchange may include replacement, recrystallization, Oswald ripening, surface diffusion, volume diffusion, grain boundary diffusion, and dislocation/lattice diffusion (e.g., Cole and Chakraborty 2001). Attainment of isotopic equilibrium in fluid-mineral systems is often difficult in experimental systems, especially at low temperatures, where the rates of diffusion are very low. Determination of equilibrium isotopic partitioning is of particular interest because equilibrium fractionation factors provide insights into bonding environments and other physico-chemical properties of the species of interest and equilibrium isotope fractionation factors are independent of kinetic issues or pathways of formation.

Fluid-mineral fractionation factors

In addition to providing the means for calculating the isotopic compositions of ancient fluids based on analysis of minerals, mineral-fluid isotope fractionation factors provide an opportunity to combine fractionation factors when there is a common substance such as water. A fundamental strategy for compiling databases for isotopic fractionation factors is to reference such factors to a common substance (e.g., Friedman and O'Neil 1977). For example, the quartz-water fractionation factor may be combined with the calcite-water fractionation factor to obtain the quartz-calcite fractionation factor at some temperature. It is now recognized, however, that the isotopic activity ratio of water in a number of experimental determinations of $^{18}O/^{16}O$ mineral-fluid fractionation factors has been variable, in part due to dissolution of mineral components at elevated temperature and pressure. The influence of solute composition on mineral-fluid fractionation factors may be quite significant, and this effect has been termed the *isotope salt effect* (e.g., O'Neil and Truesdell 1991; Horita et al. 1993a,b; Hu and Clayton 2003). Using substances other than water as the exchange medium is one approach to

addressing this issue. Carbonate (Clayton et al. 1989), CO_2 (O'Neil and Epstein 1966; Mattey et al. 1990; Matthews et al. 1994; Fayek and Kyser 2002), and H_2 (Vennemann and O'Neil 1996) have been used successfully. In the case of $^{18}O/^{16}O$ fractionation factors for minerals of wide geologic interest, it is generally accepted that use of carbonate as the exchange medium offers a superior reference compared to water (e.g., Clayton et al. 1989; Chacko et al. 1996; Hu and Clayton 2003). Alternatively, mineral-mineral fractionation factors may be obtained in three-phase systems that contain two minerals and water, where the isotopic effect of dissolved components in the fluid cancels out (Hu and Clayton 2003). As new isotopic systems are developed, it seems likely that a variety of reference exchange media will be required, depending on the element, as databases of fractionation factors are developed.

The significant effects on $^{18}O/^{16}O$ fractionations due to dissolved components in mineral-water systems, up to 2‰ in high-temperature experiments, highlight the importance of speciation and activity in experimental systems in terms of their effects on isotopic fractionation factors. Thermodynamic data bases (e.g., Johnson et al. 1992; Shock et al. 1997; Sverjenski et al. 1997; Holland and Powell 1998) demonstrate that for all of the elements discussed in this volume, as well as many others, speciation in aqueous solutions may be highly variable, suggesting that the *isotope salt effects* that have been observed for oxygen in mineral-water systems are likely to be much greater for metals and halogens in mineral-fluid systems; indeed, calculated isotopic fractionation factors are, in general, highly variable among various aqueous species for metals and halogens, as reviewed in Chapter 3 (Schauble 2004). As the experimental databases for isotopic fractionation factors expand for the *non-traditional* stable isotope systems, the choices of exchange media for determining isotopic fractionation factors will be critical, as will consideration of the exact species involved.

Evaluating approach toward isotopic equilibrium in experiments

In this last section, we briefly review some of the methods that have been used to evaluate isotopic exchange in experiments, highlighting approaches used in well-studied systems such as oxygen, and note some new applications in the *non-traditional* stable isotopes. One classic method for determining equilibrium fractionation factors is to approach isotopic equilibrium from both sides (O'Neil 1986b). Alternatively, assessment of isotopic equilibrium may be done using the *three isotope method* (Matsuhisa et al. 1978, 1979; Matthews et al. 1983a,b). This approach involves starting materials that lie on two separate, but parallel, mass-dependent fractionation lines, where movement toward isotopic equilibrium will move the phases onto a new mass-dependent fractionation line at an intermediate position in a ratio-ratio diagram (Fig. 10). In its application to oxygen isotopes, the $^{18}O/^{16}O$ ratios of the starting materials have been chosen to lie close to those expected under equilibrium, whereas the $^{17}O/^{16}O$ ratios may be chosen to be far from equilibrium, providing a sensitive measure of the approach to isotopic equilibrium (Fig. 10). The *three isotope method* remains one of the most elegant and rigorous means for constraining the approach toward isotopic equilibrium, and is ideally suited for isotope systems where two isotope ratios may be determined independently.

In principle, the three isotope method may be widely applied to new isotope systems such as Mg, Ca, Cr, Fe, Zn, Se, and Mo. Unlike isotopic analysis of purified oxygen, however, isotopic analysis of metals that have been separated from complex matrices commonly involves measurement of several isotopic ratios to monitor potential isobars, evaluate the internal consistency of the data through comparison with mass-dependent fractionation relations (e.g., Eqn. 8 above), or use in double-spike corrections for instrumental mass bias (Chapter 4; Albarède and Beard 2004). For experimental data that reflect partial isotopic exchange, their isotopic compositions will not lie along a mass-dependent fractionation line, but will instead lie along a line at high angle to a mass-dependent relation (Fig. 10), which will limit the use of multiple isotopic ratios for isobar corrections, data quality checks, and double-spike corrections.

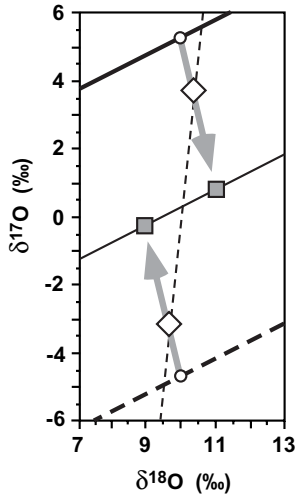

Figure 10. Three isotope method for assessing attainment of isotopic equilibrium for O isotope exchange experiments, based on the approach taken by Matthews et al. (1983a,b). Heavy solid black line (top line) reflects the terrestrial fractionation line for $^{17}O/^{16}O$-$^{18}O/^{16}O$ variations, and the small open circle on this line represents a natural mineral sample. The lower heavy dashed line represents a fluid that lies below the terrestrial fractionation line that was obtained through mixing of two highly disparate isotope compositions (MEOW II water developed at the University of Chicago). Movement of the two phases toward isotopic equilibrium will be occur in the directions of the arrows; assuming equal proportions of oxygen in the fluid and mineral phases, isotopic equilibrium will be marked by data that lie in the middle (thin solid line), where the final isotopic compositions of fluid and mineral are separated by the equilibrium fractionation factor. Partial exchange will produce isotopic compositions (diamonds) that do not lie along a mass-dependent fractionation line, where mineral-fluid pairs will define a line (dashed thin line) that lies at a high angle to a mass-dependent line.

An alternative to the three isotope method is to use an enriched isotope tracer in experiments that are run in parallel to those involving "normal" isotope compositions under identical run conditions. Use of enriched isotope tracers to evaluate the kinetics of isotopic exchange has a long history (e.g., Mills and Urey 1940). The extent of exchange toward isotopic equilibrium may be defined as:

$$F = (\delta^i E - \delta^i E_I)/(\delta^i E_E - \delta^i E_I) \tag{18}$$

where $\delta^i E_I$ and $\delta^i E_E$ are the initial and equilibrium isotopic compositions, respectively, and $\delta^i E$ is the isotopic composition observed at any time of interest (e.g., Criss et al. 1987). The fraction of isotopic exchange (F) varies from 0 to 1 as isotopic equilibrium is approached. Inspection of Equation (18) shows that F may be calculated with great sensitivity if enriched isotope tracers are used because the differences in the δ values will be large. Moreover, calculation of F using enriched isotope tracers will be relatively insensitive to the final equilibrium fractionation factor, which may be unknown at the start of an experiment. Calculation of F using Equation (18) is valid for ranges in $\delta^i E$ values up to a few hundred per mil. For more extreme isotopic enrichments, F must be calculated using the atomic abundances and molecular weights of the two components:

$$F = \frac{W_N\left(X_S^i - R_{MEAS}^{i/j} X_S^j\right)}{W_S\left(R_{MEAS}^{i/j} X_N^j - X_N^i\right) + W_N\left(X_S^i - R_{MEAS}^{i/j} X_S^j\right)} \tag{19}$$

where W_N and W_S are the molecular weights of the normal and isotopically enriched element, respectively, X^i_S and X^j_S are the atomic abundances of isotopes i and j in the isotopically enriched "spike", respectively, and X^i_N, and X^j_N are the atomic abundances of isotopes i and j for the isotopically "normal" component, respectively. Equation (19) may be derived from standard two-component mixing relations (e.g., Albarède 1995).

Substituting F into a general rate equation produces:

$$\frac{-d(1-F)}{dt} = k_n(1-F)^n \tag{20}$$

where k is the rate constant, and n is the order of the reaction, generally an integer from 0 to 3. Although most isotope exchange reactions appear to follow a first-order rate law ($n = 1$) (e.g., Criss et al. 1987; Chacko et al. 2001), isotopic exchange may also follow a second-order rate law (e.g., Graham 1981; Johnson et al. 2002). Integration of equation 20 for first- and second-order rate laws ($n = 1$ and 2) yields the following linear forms:

$$\ln(1-F) = -k_1 t \quad \text{for } n = 1 \tag{21}$$

$$\frac{F}{(1-F)} = k_2 t \quad \text{for } n = 2 \tag{22}$$

An example using enriched isotope tracers to study the kinetics of isotopic exchange is shown in Figure 11, where an enriched ^{57}Fe tracer for the ferric Fe phase was used to determine the kinetics of isotopic exchange between aqueous ferric and ferrous Fe. In the system $[Fe^{III}(H_2O)_6]^{3+}$–$[Fe^{II}(H_2O)_6]^{2+}$, Fe isotope equilibrium is rapidly attained, where 95% isotopic equilibrium is established within ~60 seconds at 22°C (Fig. 11), or within ~5 minutes at 0°C, where isotopic exchange occurs via a second-order rate law. Despite the rapid exchange kinetics, the ferric Fe species was separated essentially instantaneously, effectively "freezing in" the isotopic composition of hexaquo Fe(III) and Fe(II), with minimal isotopic re-equilibration (~10–20%) during species separation (Johnson et al. 2002; Welch et al. 2003). If the timescale of species separation was on the order of that required for isotopic equilibrium between aqueous species, the measured isotopic compositions of the separated components would *not* preserve the instantaneous compositions in solution. For the range in isotopic compositions shown in Figure 11, calculation of F for the rate equations using Equation (18) produces an error of less than 0.005 relative to that calculated using Equation (19), which is insignificant.

Although closed-system isotopic equilibrium often may be attained among aqueous species at low temperatures on reasonable timescales (Fig. 11), it is much more difficult to reach isotopic equilibrium in fluid-mineral systems at low temperatures (a few hundred degrees or less). Solid-state diffusion rates at low temperatures are far too slow to allow isotopic equilibrium to be established through diffusion alone, and instead can only occur in low-temperature experiments through recrystallization (e.g., O'Neil 1986b; Chacko et al. 2001; Cole and Chakraborty 2001). Alternatively, estimates of mineral-fluid isotope fractionation factors via direct mineral synthesis through slow precipitation is an approach many workers have taken, particularly for carbonates and oxides (e.g., O'Neil et al. 1969; Tarutani et al. 1969; Yapp 1987, 1990; Carothers et al. 1988; Kim and O'Neil 1997; Bao and Koch 1999). It is, however, recognized that the high activation energies that are associated with

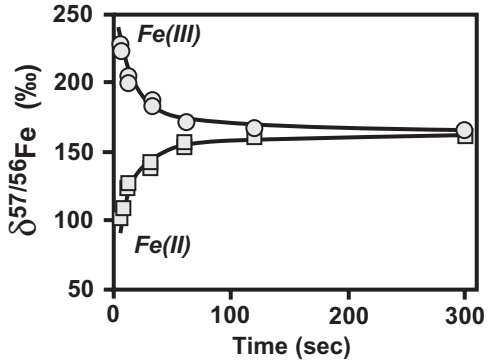

Figure 11. Determination of ferrous-ferric isotope exchange kinetics in dilute aqueous solutions using ^{57}Fe-enriched tracer solutions. Measured $\delta^{57/56}$Fe values for ferrous (squares) and ferric (circles) Fe in solution versus time. Initial $\delta^{57/56}$Fe values for $Fe(II)_{aq}$ ~0‰ and $Fe(III)_{aq}$ ~331‰. The rapid convergence in ^{57}Fe/^{56}Fe ratios for the ferric and ferrous species indicates that isotopic equilibrium is attained within minutes. Adapted from Welch et al. (2003).

nucleation and crystal growth at low temperatures may be problematic in terms of estimating equilibrium isotope fractionation factors (Chacko et al. 2001), and these factors are a likely reason for the very wide range in isotope fractionation factors that have been measured in low-temperature experiments. For example, at room temperature, there is a 16‰ range in the experimentally determined $^{18}O/^{16}O$ fractionation factor for the magnetite-water pair (O'Neil and Clayton 1964; Becker and Clayton 1976; Blattner et al. 1983; Rowe et al. 1994; Zhang et al. 1997; Mandernack et al. 1999) and a 11‰ range for the hematite-water and goethite-water pairs (Clayton and Epstein 1961; Clayton 1963; Yapp 1987, 1990; Müller 1995; Bao and Koch 1999). The rate of precipitation of minerals from solution has long been known to influence isotopic fractionations for the light stable isotopes (e.g., Turner 1982; McConnaughey 1989; Romanek et al. 1992; Kim and O'Neil 1997), and point to the importance of kinetic effects during mineral synthesis or precipitation approaches to determining isotopic fractionation factors.

Recrystallization of minerals or precursor phases may promote isotopic exchange with a fluid (e.g., O'Neil and Taylor 1967; Matthews et al. 1983a,b; Bao and Koch 1999), and will often move minerals closer to isotopic equilibrium. Qualitative evidence for dissolution/re-precipitation in experimental runs is often found in SEM or TEM images, but such images do not quantify the amount of an element that has passed through the aqueous and solid phases during dissolution/re-precipitation. Ion-microprobe analysis may identify dissolution and re-precipitation and may allow determination of isotope fractionation factors for systems that have only partially exchanged (e.g., Fortier et al. 1995). Another approach to quantifying the extent of dissolution and re-precipitation is through use of enriched isotopic tracers that are added following initial mineral formation in synthesis experiments. An example of this approach is shown in Figure 12, where an ^{57}Fe-enriched tracer was used to calculate the degree of dissolution and re-precipitation in the system $[Fe^{III}(H_2O)_6]^{3+}$–Fe_2O_3. This system was in approximate chemical equilibrium based on the observation that little change in aqueous Fe(III) contents occurred, demonstrating that the temporal changes in Fe isotope compositions reflect isotopic exchange during dissolution and re-precipitation where their relative rates were in balance; if such rates were slow, they should approach equilibrium conditions in terms of isotopic fractionation.

CONCLUSIONS

The principles of isotopic fractionation apply to all elements, and the methodologies that have been developed for the *traditional* isotopic systems such as H, C, O, and S are completely applicable to "new" isotopic systems, such as those discussed in this volume. Issues of nomenclature and standards will continue to be important as additional isotopic systems are explored, requiring the worker interested in these systems to be aware of differences among various studies that have yet to sort themselves out. Advances in theory and analytical methods promise to add many more isotopic systems to the field of *stable isotope geochemistry* than those reviewed in this volume. In addition to determining the ranges in isotopic compositions that may exist in natural systems, equal effort must be applied to experimental determination of isotope fractionation factors in carefully designed and implemented experimental studies, drawing upon the lessons that have been learned from several decades of study in the *traditional* stable isotope systems.

ACKNOWLEDGMENTS

Robert Criss, James O'Neil, and John Valley kindly reviewed the chapter. In addition, we thank the authors of the other chapters in this volume for their suggestions and comments.

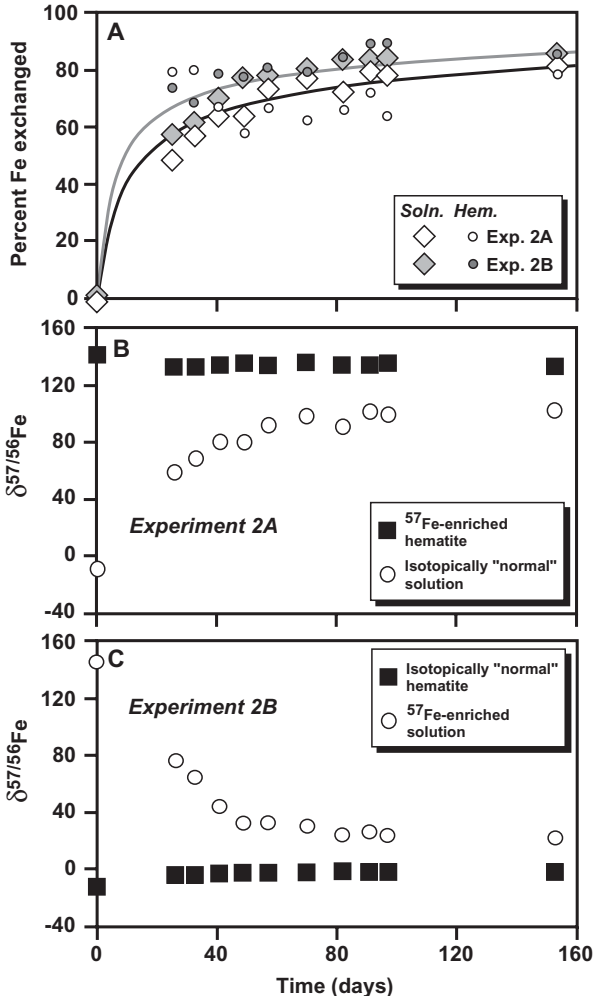

Figure 12. Extent of dissolution and re-precipitation between aqueous Fe(III) and hematite at 98°C calculated using ^{57}Fe-enriched tracers. **A.** Percent Fe exchanged (*F* values) as calculated for the two enriched-^{57}Fe tracer experiments in parts B and C. Large diamonds reflect *F* values calculated from isotopic compositions of the solution. Small circles reflect *F* values calculated from isotopic compositions of hematite, which have larger errors due to the relatively small shifts in isotopic composition of the solid (see parts B and C). Curves show third-order rate laws that are fit to the data from the solutions. **B.** Tracer experiment using ^{57}Fe-enriched hematite, and "isotopically normal" Fe(III). **C.** Identical experiment as in part B, except that solution Fe(III) is enriched in ^{57}Fe, and initial hematite had "normal" isotope compositions. Data from Skulan et al. (2002).

REFERENCES

Albarède F (1995) Introduction to Geochemical Modeling. Cambridge University Press, Cambridge, UK

Albarède F (2004) The stable isotope geochemistry of copper and zinc. Rev Mineral Geochem 55:409-427

Albarède F, Beard BL (2004) Analytical methods for non-traditional isotopes. Rev Mineral Geochem 55: 113-151

Anbar AD (2004) Molybdenum stable isotopes: observations, interpretations and directions. Rev Mineral Geochem 55:429-454

Bao H, Koch PL (1999) Oxygen isotope fractionation in ferric oxide-water systems: low-temperature synthesis. Geochim Cosmochim Acta 63:599-613

Barling J, Anbar AD (2004) Molybdenum isotope fractionation during adsorption by manganese oxides. Earth Planet Sci Lett 217:315-329

Becker RH, Clayton RN (1976) Oxygen isotope study of a Precambrian banded iron-formation. Hamersley Range, Western Australia. Geochim Cosmochim Acta 40:1153-1165

Beard BL, Johnson CM (2004) Fe isotope variations in the modern and ancient earth and other planetary bodies. Rev Mineral Geochem 55:319-357

Bigeleisen J, Mayer MG (1947) Calculation of equilibrium constants for isotopic exchange reactions. J Phys Chem 13:261-267

Birck JL (2004) An overview of isotopic anomalies in extraterrestrial materials and their nucleosynthetic heritage. Rev Mineral Geochem 55:25-64

Blattner P, Braithwaite WR, Glover RB (1983) New evidence on magnetite oxygen isotope geothermometers at 175°C and 112°C in Wairakei steam pipelines (New Zealand). Isotope Geosci 1:195-204

Bottinga Y, Javoy M (1975) Oxygen isotope partitioning among the minerals and triplets in igneous and metamorphic rocks. Rev Geophys Space Phys 13:401-418

Canfield DE (2001) Biogeochemistry of sulfur isotopes. Rev Mineral Geochem 43:607-636

Carothers WW, Adami LH, Rosenbauer RJ (1988) Experimental oxygen isotope fractionation between siderite-water and phosphoric acid liberated CO_2-siderite. Geochim Cosmochim Acta 52:2445-2450

Chacko T, Hu X, Mayeda TK, Clayton RN, Goldsmith JR (1996) Oxygen isotope fractionations in muscovite, phlogopite, and rutile. Geochim Cosmochim Acta 60:2595-2608

Chacko T, Cole DR, Horita J (2001) Equilibrium oxygen, hydrogen and carbon isotope fractionation factors applicable to geologic systems. Rev Mineral Geochem 43:1-81

Clayton RN (1963) High-temperature isotopic thermometry. *In:* Nuclear Geology on Geothermal Areas. Cons Naz Ric Lab Geol Nucl, p 222-229

Clayton RN, Epstein S (1961) The use of oxygen isotopes in high-temperature geological thermometry. J Geol 69:447-452

Clayton RN, Goldsmith JR, Mayeda TK (1989) Oxygen isotope fractionation in quartz, albite, anorthite, and calcite. Geochim Cosmochim Acta 53:725-733

Cole DR, Chakraborty S (2001) Rates and mechanisms of isotopic exchange. Rev Mineral Geochem 43:83-223

Criss RE (1999) Principles of Stable Isotope Distribution. Oxford Univ Press, New York

Criss RE, Gregory RT, Taylor HP (1987) Kinetic theory of oxygen isotope exchange between minerals and water. Geochim Cosmochim Acta 51:1099-1108

DePaolo DJ (2004) Calcium isotopic variations produced by biological, kinetic, radiogenic and nucleosynthetic processes. Rev Mineral Geochem 55:255-288

Eiler JM, Baumgartner LP, Valley JW (1992) Intercrystalline stable isotope diffusion: a fast grain boundary model. Contrib Mineral Petrol 112:543-557

Ellis AS, Johnson TM, Bullen TD (2002) Cr isotopes and the fate of hexavalent chromium in the environment. Science 295:2060-2062

Farquhar J, Bao H, Thiemens M (2000) Atmospheric influence of Earth's earliest sulfur cycle. Science 289: 756-758

Fayek M, Kyser TK (2000) Low temperature oxygen isotopic fractionation in the uraninite-UO_3-CO_2-H_2O system. Geochim Cosmochim Acta 64:2185-2197

Fortier SM, Cole DR, Wesolowski DJ, Riciputi LR, Paterson BA, Valley JW, Horita J (1995) Determination of the magnetite-water equilibrium oxygen isotope fractionation factor at 350°C: a comparison of ion microprobe and laser fluorination techniques. Geochim Cosmochim Acta 59:3871-3875

Friedman I, O'Neil JR (1977) Compilation of Stable Isotope Fractionation Factors of Geochemical Interest. US Geol Surv Prof Paper 440-KK

Giletti BJ (1986) Diffusion effects on oxygen isotope temperatures of slowly cooled igneous and metamorphic rocks. Earth Planet Sci Lett 77:218-228

Graham CM (1981) Experimental hydrogen isotope studies. Diffusion of hydrogen in hydrous minerals, and stable isotope exchange in metamorphic rocks. Contrib Mineral Petrol 76:216-228

Hoefs J (2004) Stable isotope geochemistry. 5th Edition. Springer, Berlin

Holland TJB, Powell R (1998) An internally consistent thermodynamic data set for phases of petrological interest. J Metamorphic Geology 16:309-343

Horita J, Wesolowski DJ, Cole DR (1993a) The activity-composition relationship of oxygen and hydrogen isotopes in aqueous salt solution: I. Vapor-liquid water equilibration of single salt solutions for 50 to 100°C. Geochim Cosmochim Acta 57:2797-2817

Horita J, Cole DR, Wesolowski DJ (1993b) The activity-composition relationship of oxygen and hydrogen isotopes in aqueous salt solution: II. Vapor-liquid water equilibration of mixed salt solutions from 50 to 100°C and geochemical implications. Geochim Cosmochim Acta 57:4703-4711

Hu G, Clayton RN (2003) Oxygen isotope salt effects at high pressure and high temperature and the calibration of oxygen isotope geothermometers. Geochim Cosmochim Acta 67:3227-3246

Jackson TA (2001) Variations in the isotope composition of mercury in a freshwater sediment sequence and food web. Canadian J Fish Aquat Sci 58:185-196

Johnson CM, Skulan JL, Beard BL, Sun H, Nealson KH, Braterman PS (2002) Isotopic fractionation between Fe(III) and Fe(II) in aqueous solutions. Earth Planet Sci Lett 195:141-153

Johnson CM, Beard BL, Roden EE, Newman DK, Nealson KH (2004) Isotopic constraints on biogeochemical cycling of Fe. Rev Mineral Geochem 55:59-408

Johnson JM, Oelkers EH, Helgeson HC (1992) SUPRT92: A software package for calculating the standard molal thermodynamic properties of minerals, gases, aqueous species and reactions from 1 to 5000 bars and 0 to 1000°C. Comput Geosci 18:899-947

Johnson TM, Bullen TD (2004) Mass-dependent fractionation of selenium and chromim isotopes in low-temperature environments. Rev Mineral Geochem 55:289-317

Kim S-T, O'Neil JR (1997) Equilibrium and nonequilibrium oxygen isotope effects in synthetic carbonates. Geochim Cosmochim Acta 61:3461-3475

Kohn MJ, Valley JW (1998) Obtaining equilibrium oxygen isotope fractionations from rocks: theory and example. Contrib Mineral Petrol 132:209-224

Lide DR (2003) CRC handbook of chemistry and physics (84th ed). CRC press, Boca Raton

Mandernack KW, Bazylinski DA, Shanks WC III, Bullen TD (1999) Oxygen and iron isotope studies of magnetite produced by magnetotactic bacteria. Science 285:1892-1896

Matsuhisa Y, Goldsmith JR, Clayton RN (1978) Mechanisms of hydrothermal crystallization of quartz at 250°C and 15 Kbar. Geochim Cosmochim Acta 42:173-182

Matsuhisa Y, Goldsmith JR, Clayton RN (1979) Oxygen isotopic fractionation in the system quartz-albite-anorthite-water. Geochim Cosmochim Acta 43:1131-1140

Mattey DP, Taylor WR, Green DH, Pillinger CT (1990) Carbon isotopic fractionation between CO_2 vapor, silicate and carbonate melts: An experimental study to 30 kbar. Contrib Mineral Petrol 104:492-505

Matthews A, Goldsmith JR, Clayton RN (1983a) Oxygen isotope fractionations involving pyroxenes: The calibration of mineral-pair geothermometers. Geochim Cosmochim Acta 47:631-644

Matthews A, Goldsmith JR, Clayton RN (1983b) On the mechanisms and kinetics of oxygen isotope exchange in quartz and feldspars at elevated temperatures and pressures. Geol Soc Am Bull 94:396-412

Matthews A, Palin JM, Epstein S, Stolper EM (1994) Experimental study of $^{18}O/^{16}O$ partitioning between crystalline albite, albitic glass, and CO_2 gas. Geochim Cosmochim Acta 58:5255-5266

McConnaughey T (1989) ^{13}C and ^{18}O isotopic disequilibrium in biological carbonates: I. Patterns. Geochim Cosmochim Acta 53:151-162

Mills GA, Urey HC (1940) The kinetics of isotopic exchange between carbon dioxide, bicarbonate iron, carbonate ion and water. J Am Chem Soc 62:1019-1026

Müller J (1995) Oxygen isotopes in iron (III) oxides: A new preparation line; mineral-water fractionation factors and paleo-environmental considerations. Isotopes Environ Health Stud 31:301-302

O'Neil JR (1986a) Appendix: Terminology and Standards. Rev Mineral 16:561-570

O'Neil JR (1986b) Theoretical and experimental aspects of isotopic fractionation. Rev Mineral 16:1-40

O'Neil JR, Clayton RN (1964) Oxygen isotope geothermometry. *In:* Isotope and Cosmic Chemistry. Craig H, Miller SL, Wasserburg GW (eds) North-Holland, Amsterdam, p 157-168

O'Neil JR, Epstein S (1966) Oxygen isotope fractionation in the system dolomite-calcite-carbon dioxide. Science 152:198-201

O'Neil JR, Taylor Jr HP (1967) The oxygen isotope and cation exchange chemistry of feldspar. J Geophys Res 74:6012-6022

O'Neil JR, Truesdell AH (1991) Oxygen isotope fractionation studies of solute-water interactions. *In:* Stable Isotope Geochemistry: A Tribute to Samuel Epstein. Taylor Jr. HP, O'Neil JR, Kaplan IR (eds), Geochem Soc Spec Pub 3:17-25

O'Neil JR, Clayton RN, Mayeda TK (1969) Oxygen isotope fractionation in divalent metal carbonates. J Chem Phys 51:5547-5558

Polyakov VB, Mineev SD (2000) The use of Mössbauer spectroscopy in stable isotope geochemistry. Geochim Cosmochim Acta 64:849-865

Rayleigh L (1902) On the distillation of binary mixtures. Phil Mag S.6 4:521-537

Rehkämper M, Halliday AN (1999) The precise measurement of Tl isotopic compositions by MC-ICP-MS: application to the analysis of geological materials and meteorites. Geochim Cosmochim Acta 63:935-944

Rehkämper M, Frank M, Hein JR, Porcelli D, Halliday A, Ingri J, Liebetrau V (2002) Thallium isotope variations in seawater and hydrogenetic, diagenetic, and hydrothermal ferromanganese deposits. Earth Planet Sci Lett 197:65-81

Romanek CS, Grossman EL, Morse JW (1992) Carbon isotopic fractionation in synthetic aragonite and calcite: Effects of temperature and precipitation rate. Geochim Cosmochim Acta 56:419-430

Rowe MW, Clayton RN, Mayeda TK (1994) Oxygen isotopes in separated components of CI and CM meteorites. Geochim Cosmochim Acta 58:5341-5347

Schauble EA (2004) Applying stable isotope fractionation theory to new systems. Rev Mineral Geochem 55: 65-111

Schauble EA, Rossman GR, Taylor Jr. HP (2001) Theoretical estimates of equilibrium Fe-isotope fractionations from vibrational spectroscopy. Geochim Cosmochim Acta 65:2487-2497

Schauble EA, Rossman GR, Taylor Jr. HP (2003) Theoretical estimates of equilibrium chlorine-isotope fractionations. Geochim Cosmochim Acta 67:3267-3281

Schauble EA, Rossman GR, Taylor Jr. HP (2004) Theoretical estimates of equilibrium chromium-isotope fractionations. Chem Geol, in press.

Shock EL, Sassani DC, Willis M, Sverjensky DA (1997) Inorganic species in geologic fluids: Correlations among standard molal thermodynamic properties of aqueous cations and hydroxide complexes. Geochim Cosmochim Acta 61:907-950

Skulan JL, Beard BL, Johnson CM (2002) Kinetic and equilibrium Fe isotope fractionation between aqueous Fe(III) and hematite. Geochim Cosmochim Acta 66:2995-3015

Stewart MA, Spivack AJ (2004) The stable-chlorine isotope compositions of natural and anthropogenic materials. Rev Mineral Geochem 55:231-254

Sverjensky DA, Shock EL, Helgeson HC (1997) Prediction of the thermodynamic properties of aqueous metal complexes to 1000°C and 5 kb. Geochim Cosmochim Acta 61:1359-1412

Tarutani T, Clayton RN, Mayeda TK (1969) The effect of polymorphism and magnesium substitution on oxygen isotope fractionation between calcium carbonate and water. Geochim Cosmochim Acta 33: 987-996

Tomascak PB (2004) Developments in the understanding and application of lithium isotopes in the earth and planetary sciences. Rev Mineral Geochem 55:153-195

Turner JV (1982) Kinetic fractionation of carbon-13 during calcium carbonate precipitation. Geochim Cosmochim Acta 46:1183-1191

Urey HC (1947) The thermodynamic properties of isotopic substances. J Chem Soc (London), p 562-581

Valley JW, Cole DR (eds) (2001) Stable Isotope Geochemistry. Rev Mineral Geochem, Vol 43

Valley JW, Taylor HP Jr, O'Neil JR (eds) (1986) Stable Isotopes in High Temperature Geological Processes. Rev Mineral, Vol 16

Vennemann TW, O'Neil JR (1996) Hydrogen isotope exchange between hydrous minerals and molecular hydrogen: I. A new approach for the determination of hydrogen isotope fractionation at moderate temperature. Geochim Cosmochim Acta 60:2437-2451

Welch SA, Beard BL, Johnson CM, Braterman PS (2003) Kinetic and equilibrium Fe isotope fractionation between aqueous Fe(II) and Fe(III). Geochim Cosmochim Acta 67:4231-4250

Yapp CJ (1987) Oxygen and hydrogen isotope variations among goethites (FeOOH) and the determination of paleotemperatures. Geochim Cosmochim Acta 51:355-364.

Yapp CJ (1990) Oxygen Isotopes in iron (III) oxides 1. Mineral-water factors. Chem Geol 85:329-335

Young ED, Galy A (2004) The isotope geochemistry and cosmochemistry of magnesium. Rev Mineral Geochem 55:197-230

Zhu XK, O'Nions RK, Guo Y, Reynolds BC (2000) Secular variation of iron isotopes in north Atlantic Deep Water. Science 287:2000-2002.

Zhang C, Liu S, Phelps TJ, Cole DR, Horita J, Fortier SM, Elless M, Valley JW (1997) Physiochemical, mineralogical, and isotopic characterization of magnetite-rich iron oxides formed by thermophilic iron-reducing bacteria. Geochim Cosmochim Acta 61:4621-4632